Covalent Attachment of Gold Nanoparticles to DNA Templates

Karen A. Stevenson, G. Muralidharan, Leon Maya[1], Jack C. Wells[2], Jacob Barhen[2], Thomas Thundat*
Center for Engineering Science Advanced Research, Life Sciences Division, [1]Chemical Sciences Division, [2]Computer Science and Mathematics Division, Oak Ridge National Laboratory, Oak Ridge, TN 37831

Abstract

Functionalized gold nanoparticles have been covalently bound to internal, modified sites on double-stranded DNA. Gold nanoparticles coated with mercaptosuccinic acid or thioctic acid were bound to amino-modified thymine bases on double-stranded DNA. Visible absorbance spectra, gel electrophoresis, and atomic force microscopy were used to analyze the products. Thiol groups were added to one end of the gold/nanoparticle product, which was then attached to a gold surface. This method has the potential to allow controlled placement of particles with sub-nanometer precision and to allow attachment of the product to fixed contacts for nanodevice fabrication.

Covalent Attachment of Gold Nanoparticles to DNA Templates

Karen A. Stevenson, G. Muralidharan, Leon Maya[1], Jack C. Wells[2], Jacob Barhen[2], Thomas Thundat*
Center for Engineering Science Advanced Research, Life Sciences Division, [1]Chemical Sciences Division, [2]Computer Science and Mathematics Division, Oak Ridge National Laboratory, Oak Ridge, TN 37831

The ability to assemble nanoparticles into arrays, networks, and circuits in a precise and controlled manner is key to the fabrication of a variety of nanodevices. Networks of nanometer–sized metal or semiconductor islands, or quantum dots, may exhibit a variety of quantum phenomena, with applications in optical devices [1], nanometer-sized sensors [2], advanced computer architectures [3], ultradense memories [4], and quantum-information science and technology. [5-7] The challenge is that fabrication with nanoscale precision of nanoparticle arrays in a time and cost effective manner remains a formidable task. At present, particle-based and e-beam lithography lack the required resolution. Scanning probe microscopy can be used for making molecular devices, but it is slow and impractical for mass production. A variety of other techniques have been demonstrated, including self-assembled monolayers [8], block copolymer template lithography [9] or electrodeposition [10], and controlled deposition by cleaved edge overgrowth.[11] All of these techniques have limitations on the size of the particle and/or the pattern of the resulting array.

*Corresponding Author

Interest in the concept of self-assembled nanostructures led to the idea of using DNA as a scaffold or template for the programmed assembly of nanoscale arrays (see review by Storhoff and Mirkin [12]). Beginning in the 1980's, Seeman et al. experimented with combining DNA fragments to produce geometrical shapes, including cubes [13], triangles [14], two-dimensional arrays [15-17] and various forms of DNA knots. [18-19] Recently, LaBean, Seeman, et al. have continued this work with the construction of triple crossover complexes.[20] This work has pioneered the concept of using DNA as a structural molecule, which offers many advantages compared to other homopolymers. DNA can be easily synthesized in lengths up to 40 nm and double-stranded DNA can be joined end to end to produce longer linear molecules or more complex shapes. It can be modified with functional groups at predetermined sites to allow for the attachment of other molecules in a specific manner.

DNA has been used previously in the programmed assembly of nanoparticles. Mirkin et al. [21-23] and Alivisatos et al. [24-25] have successfully attached oligonucleotide-derivatized nanoparticles to DNA using hybridization techniques. Alivisatos also bound gold particles to both single-stranded and double-stranded DNA modified with thiol groups. [24] Niemeyer and coworkers conjugated streptavidin to single-stranded DNA oligonucleotides, hybridized the conjugates to a complementary RNA template, and bound biotinylated gold clusters to the streptavidin.[26] Fullerene derivatives were assembled along the phosphate groups of the DNA backbone using cation exchange by Cassell et al. [27] and Coffer and coworkers formed rings of cadmium sulfide nanoparticles using double-stranded circular plasmid DNA attached to a solid substrate.[28]

This communication describes a new approach for binding nanoparticles to DNA. Functionalized nanoparticles are covalently bound to internal, chemically modified bases on double-stranded DNA without the presence of destabilizing "nicks" along the DNA backbone. Since DNA can be synthesized with a variety of chemical modifications, this technique allows great versatility in the attachment of nanoparticles with corresponding functional groups. This method potentially allows closer spacing of very small particles than hybridization based methods, and greater precision in the placement of particles than using a plasmid or the DNA backbone as a template. In addition, we report an approach for thiolating one end of the DNA/nanoparticle product and attaching it to a gold surface. The ability to attach one or both ends of the DNA/gold complex, after generation of the desired pattern, to fixed contacts or electrodes is a necessary step in nanodevice fabrication.

Oligonucleotides were designed with amino-modified bases for attachment to carboxylic acid functionalized gold particles. Two double-stranded DNA sequences were used. They were designed with 5' overhangs to permit easy ligation. Sequence 1 DNA was 22 base pairs long with two binding sites for gold per DNA molecule. The separation between gold binding sites was 3.7 nm. Sequence 2 DNA was 30 base pairs long, had one gold binding site per DNA molecule, and, after ligation, a 10.5 nm separation between binding sites. Gold nanoparticles with two different passivating coatings were tested. Particles with an average diameter of 1.5 nm were synthesized with a mercaptosuccinic acid coating, and particles approximately 2.5 nm in size were coated with thioctic acid.[29] Each particle has multiple reactive carboxyl groups on its surface. In order to decrease the probability for one particle binding to many amino groups on the DNA, methylamine

4

was used to block some of the carboxyl groups on the gold. Methylamine was chosen for this purpose because of its small size and similarity to the methylene side chain containing the amino group on the DNA. The reaction between the amino group on the DNA and the carboxyl group on the gold particle was facilitated using a standard chemical method for joining carboxyl groups to amino groups, 1-ethyl-3-(3-dimethylaminopropyl) carbodiimide hydrochloride (EDC) and N-hydroxysuccinimide (NHS). EDC is used to activate carboxyl groups and NHS stabilizes the active amine-reactive intermediate. Addition of an amino-containing compound results in the formation of an amide bond.[30-31]   Analysis of the products by gel electrophoresis and atomic force microscopy (AFM) showed the gold particles bound to the DNA. In addition, absorbance spectra of the gold nanoparticles in the presence of DNA provide evidence of binding.

Absorbance spectrum data for thioctic acid gold particles and Sequence 1 DNA is shown in Figure 1. Figure 1A shows the spectrum of gold particles that were not activated with EDC and NHS and spectra of the untreated particles incubated with DNA. All the samples had the same concentration of gold particles, 43 μg/ml. Since the concentration of gold is the same for all the spectra, the expected result is that all the spectra should overlap. From top to bottom, the top broken line represents overlapping spectra of gold particles incubated with 123 and 185 pmol of gold binding sites on the DNA The dashed line is the spectrum of gold incubated with 62 pmol binding sites. The dotted line represents gold particles incubated with 31 pmol binding sites, and the solid line is the spectrum of gold particles alone. No significant differences are observed in the spectra of the gold particles incubated with DNA versus the gold particles alone.

Figure 1B shows the visible absorbance spectra of gold nanoparticles treated with EDC

and NHS to activate the carboxyl groups, and activated particles that were incubated with

various amounts of DNA. The concentration of gold was the same in all samples, 63

μg/ml. From top to bottom, the solid black spectrum represents activated gold particles

alone, the dotted line gold particles incubated with 36 pmol of gold binding sites on the

DNA, the short dashed line gold and 74 pmol of binding sites, the medium dashed line

gold plus 111 pmol of binding sites, and the bottom broken line gold incubated with 185

pmol of binding sites. In contrast to the control experiment shown in Figure 1A, there is

a significant hypochromic effect when the gold binds to the DNA and the absorbance

peak of the particles shifts to a longer wavelength after incubation with DNA. The

absorbance maximum for the gold particles alone is at 514 nm while the absorbance

maximum of the spectrum with 185 pmoles of DNA binding sites occurs at 523 nm. The

hypochromicity and spectral shifts demonstrate that the gold particles are bound to the

DNA.

Gel electrophoresis was performed to confirm the spectrophotometric results. Figure 2

shows agarose gels of Sequence 1 DNA bound to the succinate-coated gold

nanoparticles. Silver staining was used to enhance the detection of gold. In Figure 2A

gold nanoparticles were pre-treated with EDC and NHS to activate the carboxyl groups,

then the particles were incubated with ligated DNA in the presence or absence of

methylamine. Lane 2 contains gold particles bound to DNA in the absence of

methylamine, and lanes 3-6 contain DNA bound to nanoparticles in the presence of

increasing amounts of methylamine. Lane 8 contains activated gold particles alone. The

gel shows that the gold particles bound to the DNA (lanes 2-6) have a reduced mobility compared to the gold particles alone. This is true both in the absence of methylamine (lane 2) as well as in the presence of methylamine. The mobility shift is due to the higher molecular weight of the gold/ DNA complex compared to the gold particles alone. In the presence of high concentrations of methylamine (lanes 5 and 6) the mobility shift is not as great as in the reactions containing lower concentrations. This represents overall reduced binding to the DNA due to fewer reactive groups on the gold particles' surfaces. Figure 2B shows the mobility of the gold particles incubated with unligated and ligated DNA without pretreatment with EDC and NHS. Lanes 3 and 4 show the DNA monomer mixed with gold and 2 different concentrations of methylamine. Lanes 6 and 7 show the ligated DNA mixed with gold and two different concentrations of methylamine, and lane 8 shows the gold particles alone. Without pretreatment of the gold particles, there is no change in the mobility of gold in the presence of DNA and methylamine.

AFM images of ligated Sequence 1 DNA bound to succinate-coated gold are shown in Figure 3. Figure 3A shows ligated Sequence 1 DNA bound to succinate-coated gold nanoparticles without using methylamine to block excess binding sites on the gold particle. An aggregate of gold particles and DNA is formed, presumably due to the multiple binding sites on the gold particles. The binding sites for the gold particles are approximately 3.7 nm apart in DNA Sequence 1. Figure 3B shows Sequence 1 DNA bound to the same gold particles in the presence of methylamine. The methylamine concentration in the reaction was equal to twice the concentration of amino-modified thymines on the DNA. Cross-linking was greatly reduced, if not eliminated completely, with the addition of methylamine. Figure 3C shows a close-up view of gold particles

bound at internal sites along several strands of DNA with the DNA clearly visible between the gold clusters (arrows). Analysis of Figure 3C shows that the average height of the DNA between gold particles (arrows) is 0.74 nm, in good agreement with published values,[32-33] while the height of the DNA bound to the particles is approximately 3 nm.

Figure 4A shows ligated Sequence 2 DNA bound to thioctic acid gold nanoparticles in the absence of methylamine. The separation between binding sites on Sequence 2 DNA is approximately 10 nm. Cross-linking between the DNA and the thioctic acid-coated gold particles did not present as much of a problem as it did with the succinate-coated gold and the DNA with a 3.7 nm separation between binding sites. Figure 4B shows a close-up of the Sequence 2 DNA bound to the thioctic acid-coated particles. It does appear at one end that there may be two double-stranded DNA molecules cross-linked by the multiple binding sites on the gold or that the DNA is folded back on itself.

Figure 5 shows thiolated Sequence 1 DNA bound to succinate-coated particles. The DNA was designed with 5' overhangs allowing the addition of thiol groups after the DNA was bound to the particles. Complementary oligonucleotides with a 3' thiol group were annealed to the overhangs in the presence of T4 DNA ligase. The advantage of thiolating the DNA after binding it to the gold particles is that thiolated DNA forms dimers in the absence of reducing reagents. The dimer and/or the reducing agents can interfere with the binding of the particles to the DNA. Dimers are also clearly visible on gels and can complicate the interpretation of mobility shift assays. A drop of DNA thiolated as described above was placed on the interface of a mica surface that had been partially

8

coated with gold. After rinsing, no DNA was observed on the mica side of the substrate, while Figure 5 shows DNA bound on the gold-coated mica. The networking seen in the image may be due to cross-linking, disulfide bond formation between DNA molecules, or may be a result of the deposition of the sample on the gold-coated mica substrate.

We have covalently attached functionalized gold nanoparticles along engineered, internal sites of double-stranded DNA molecules without the presence of "nicks" along the DNA backbone. This method of programmed assembly using DNA templates offers the potential advantage that nanoparticles can be bound wherever a modified base is inserted during synthesis of the DNA. Refinements of this technique may lead to nanoparticle assemblies whose structure is dependent only on the design of the DNA template and the size of the particle. A variety of functional groups can be used to modify DNA during synthesis and any particle that can be functionalized with a complementary reactive group can be bound to the DNA. The DNA product is double-stranded thus retaining the regularity of secondary structure that makes DNA an attractive template for nanofabrication and assembly of nanoparticles. Thiolation of the DNA after the desired product has been achieved allows greater flexibility in manipulating the DNA during the coupling process. The alternative of using DNA thiolated at one or both ends during synthesis of the DNA precludes ligation of the strands and can lead to disulfide bonds between DNA molecules.

In summary, this technique addresses a basic need to assemble nanometer-scale objects in a programmable manner and in a massively parallel fashion, from the bottom up.

References

1. D. Bimberg, M. Grundman, N. N. Ledenstov, *Quantum Dot Heterostructures*, John Wiley & Sons, New York, NY (1998).

2. A. N. Cleland, M. L. Roukes, *Nature* **392**, 160 (1998).

3. K. K. Likharev, *Proc. IEEE* **87**, 606 (1999).

4. K. K. Likharev, *Nanotechnology* **10**, 159 (1999).

5. S. Lloyd, *Science* **261**,1569 (1993).

6. S. Benjamin, *Phys. Rev. A* **61**, 020301(R) (2000).

7. D. P. DiVincenzo, *Fortschr. der Phys.* **48**, 771 (2000).

8. E. Delamarche, H. Schmid, H. A. Biebuyck, B. Michel, *Adv. Mater.* **9,** 741 (1997).

9. M. Park, C. Harrison, P. M. Chaikin, R. A. Register, D. H. Adamson, *Science* **276**, 1401 (1997).

10. T. Thurn-Albrecht, J. Schotter, G. A. Kastle, N. Emley, T. Shibauchi, L. Krusin-Elbaum, K. Guarini, C. T. Black, M. T. Tuominen, T. P. Russell, T. P. *Science* **290**, 2126 (2000).

11. G. Fasol, K. Runge, *Appl. Phys. Lett.* **70**, 2467 (1997).

12. J. J. Storhoff, C. A. Mirkin, *Chem. Rev.* **99**, 1849 (1999).

13. J. Chen, N. C. Seeman, *Nature* **350**, 631 (1991).

14. J. Qi, X. Li, X. Yang, N. C. Seeman, *J. Am. Chem. Soc.* **118**, 6121 (1996).

15. Y. Zhang, N. C. Seeman, *J. Am. Chem. Soc.* **116**, 1661 (1994).

16. X. Li, X. Yang, J. Qi, N. C. Seeman, *J. Am. Chem. Soc.* **118**, 6131 (1996).

17. E. Winfree, F. Liu, L. A. Wenzler, N. C. Seeman, *Nature* **394**, 539 (1998).

18. J. E. Mueller, S. M. Du, N. C. Seeman, *J. Am. Chem. Soc.* **113**, 6306 (1991).

19. S. M. Du, N. C. Seeman, *Biopolymers* **34**, 31 (1994).

20. T. H. LaBean, H. Yan, J. Kopatsch, F. Liu, E. Winfree, J. H. Reif, N. C. Seeman, *J. Am. Chem. Soc.* **122**, 1848 (2000).

21. C. A. Mirkin, R. L. Letsinger, R. C. Mucic, J. J. Storhoff, *Nature* **382**, 607 (1996).

22. G. P. Mitchell, C. A. Mirkin, R. L. Letsinger, *J. Am. Chem. Soc.* **121**, 8122 (1999).

23. C. A. Mirkin, *Inorg. Chem.* **39**, 2258 (2000).

24. C. J. Loweth, W. B. Caldwell, X. Peng, A. P. Alivisatos, P. G. Schultz, *Angew. Chem. Int. Ed.* **38**, 1808 (1999).

25. A. P. Alivisatos, K. P. Johnsson, X. Peng, T. E. Wilson, C. J. Loweth, M. P. Bruchez, Jr., P. G. Schultz, *Nature* **382**, 609 (1996).

26. C. M. Niemeyer, W. Burger, J. Peplies, *Angew. Chem. Int. Ed.* **37**, 2265 (1998).

27. A. M. Cassell, W. A. Scrivens, J. M. Tour, *Angew. Chem. Int. Ed.* **37**, 1528 (1998).

28. J. L. Coffer, S. R. Bigham, X. Li, R. F. Pinizzotto, Y. G. Rho, R. M. Pirtle, I. L. Pirtle, *Appl. Phys. Lett.* **69**, 3851 (1996).

29. L. Maya, G. Muralidharan, T. G. Thundat, E. A. Kenik, *Langmuir* **16**, 9151 (2000).

30. Z. Grabarek and J. Gergely, *Anal. Biochem.* **185**, 131 (1990).

31. J. V. Staros, R. W. Wright, D. M. Swingle, *Anal. Biochem.* **156**, 220 (1986).

32. T. Thundat, D. P. Allison, R. J. Warmack, *Nuc. Acids Res.* **22**, 4224 (1994).

33. W-L. Shaiu, D. D. Larson, J. Vesenka, E. Henderson, *Nuc. Acids Res.* **21**, 99 (1993).
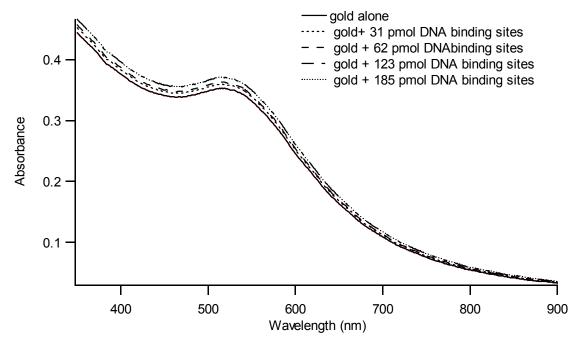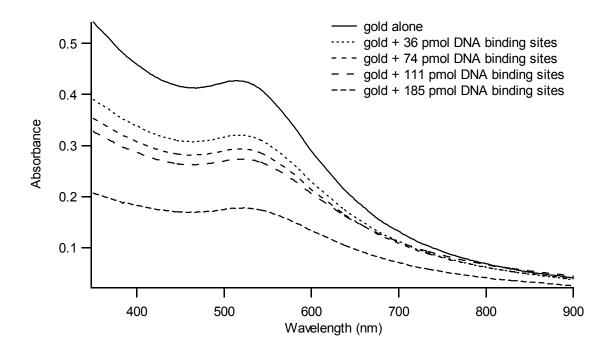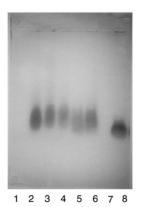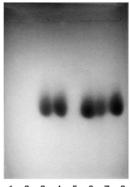
Figure 1A

Figure 1B

Figure 2A

Figure 2B

Figure 3A
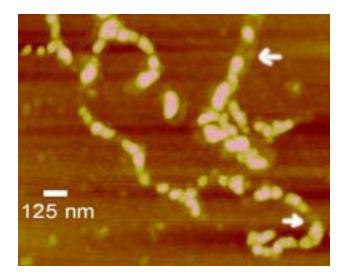

Figure 3B
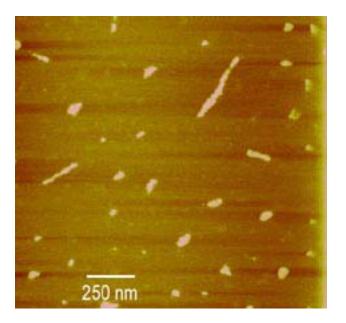
Figure 3C

Figure 4A
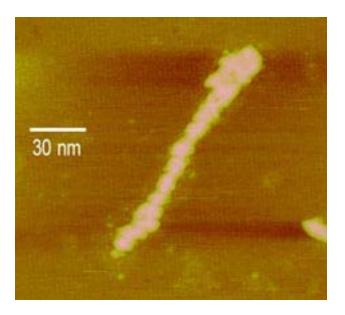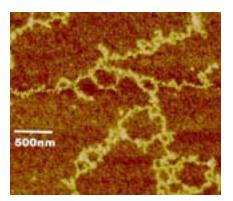
Figure 4B

Figure 5

Figure Legends

Figure 1. Visible absorbance spectra of gold particles in the presence and absence of Sequence 1 DNA. **A.** Spectra of unactivated gold particles alone and after incubation with various amounts of DNA. The concentration of gold particles in all the samples was the same, 43 μg/ml. From top to bottom: Top broken line: Overlapping spectra of gold particles incubated with 123 and 185 pmol gold binding sites on the DNA. Dashed line: Gold particles incubated with 62 pmol DNA binding sites. Dotted line: Gold particles incubated with 31 pmol binding sites. Solid line: Gold particles alone. **B.** Spectra of gold nanoparticles activated with EDC and NHS alone and after incubation with various amounts of DNA. The concentration of gold in all the samples was the same, 63 μg/ml. From top to bottom: Solid line, gold particles treated with EDC and NHS. Dotted line, treated gold particles incubated with 36 pmol gold binding sites on the DNA. Short dashed line, treated gold particles incubated with 74 pmol DNA binding sites. Medium dashed line, treated gold particles incubated with 111 pmol DNA binding sites. Bottom dashed line, treated gold particles incubated with 185 pmol DNA binding sites.

Figure 2. Agarose gel electrophoresis of Sequence 1 DNA and succinate-coated gold nanoparticles. **A.** Carboxyl groups on the gold particles were activated with EDC and NHS, then incubated with Sequence 1 ligated DNA in the presence or absence of methylamine. The gel was silver-stained to visualize gold. Lane 2: Gold particles incubated with DNA in the absence of methylamine. Lane 3-6: Gold particles incubated with DNA with increasing amounts of methylamine. Lane 3: Methylamine concentration twice the concentration of gold binding sites on the DNA. Lane 4: Methylamine concentration four times the concentration of gold binding sites. Lane 5: Methylamine concentration ten times the concentration of gold binding sites. Lane 6: Methylamine concentration twenty times the concentration of gold binding sites. Lane 8: Activated gold particles alone. **B.** Unactivated gold nanoparticles incubated with Sequence 1 unligated or ligated DNA and methylamine. Lane 3: Gold particles incubated with unligated DNA and a methylamine concentration 0.35 times the concentration of gold binding sites on the DNA. Lane 4: Gold particles incubated with DNA and a methylamine concentration 88 times the concentration of gold binding sites. Lane 6: Gold particles incubated with ligated DNA and a methylamine concentration 0.53 times the concentration of gold binding sites on the DNA. Lane 7: Gold particles incubated with DNA and a methylamine concentration 132 times the concentration of gold binding sites. Lane 8: Gold particles alone.

Figure 3. AFM images of succinate-coated gold nanoparticles bound to ligated Sequence 1 DNA on a mica substrate. Separation between gold binding sites on the DNA was approximately 3.7 nm. **A.** Carboxylic acid functionalized gold particles bound to amino-modified thymines on DNA in the absence of methylamine. **B.** Gold particles bound to DNA in the presence of methylamine. The concentration of methylamine was twice the concentration of DNA binding sites. **C.** Close-up view showing DNA between gold particles. Arrows shows the DNA. The concentration of methylamine was the same as in **B**.

Figure 4. AFM images of thioctic acid-coated gold bound to ligated Sequence 2 DNA on a mica substrate. Separation between gold binding sites on the DNA was approximately 10.5 nm. **A.** Typical products of the reaction between Sequence 2 DNA and thioctic acid-coated gold particles. **B.** Close-up view of Sequence 2 DNA bound to thioctic acid gold particles.

Figure 5. AFM image of succinate-coated gold bound to ligated Sequence 1 DNA. The DNA was thiolated after the reaction between the gold and the DNA. The substrate is gold-coated mica.

Experimental Section

Oligonucleotides were purchased from Oligos Etc. They were designed with C6-amino-modified thymines (X) and with compatible overhangs to permit ligation reactions to easily occur. Two double-stranded oligonucleotides were used. Sequence 1 had gold binding sites located approximately 3.7 nm apart:

5'-GATCTAXCAACGGCTCAXCCAA $X=T-(CH_2)_6-NH_2$
       TAGTTGCCGAGTAGGTTCTAGA-5'

Sequence 2 had gold binding sites located approximately 10.5 nm apart after ligation:

5'- GATCTAGGTCACTGXCAACGGCTCATCCAA $X=T-(CH_2)_6-NH_2$
       TCCAGTGACAGTTGCCGAGTAGGTTCTAGA-5'

For some experiments, the 5' ends of the double-stranded oligonucleotide were phosphorylated and then the DNA was ligated. Enzymes were purchased from Promega.

Gold nanoparticles coated with mercaptosuccinic acid or thioctic acid were synthesized as described elsewhere.[29] Succinate-coated gold was dissolved in water and the pH adjusted to ~3.8. Final concentration of the gold solution was 4.7 mg/ml. Approximately 50μg gold nanoparticles were incubated at room temperature with ~1.5mg 1-ethyl-3-(3-dimethylaminopropyl) carbodiimide hydrochloride (Pierce) and ~2.0mg N-hydroxysuccinimide (Pierce) for 30-60 minutes. Thioctic acid-coated gold was dissolved with shaking in water and NaOH (approximately pH 11.0) then the pH was adjusted with HCl to approximately pH 8.4. Final concentration was approximately 2.15 mg/ml.

Methylamine (Sigma) concentrations were calculated as multiples of gold binding sites on the DNA. Typical amounts used were 1X (equal to the concentration of modified thymines), 2X, 5X, 10X, and no methylamine. The methylamine was added to 2-10 μg DNA and then this mixture was added to the gold particles. Incubation was typically overnight at room temperature.

Thiolation of the DNA was performed using the oligonucleotide

5'-AGATCCX-3'   X=3'-SH $(CH_2)_3$

A 10-fold molar excess of the thiolated oligonucleotide was added to the DNA/gold product in the presence of T4 DNA ligase . The reaction was incubated overnight at room temperature.

For AFM imaging, reaction mixtures were diluted 1:10,000 to 1:20,000 in 20mM Tris, 5mM KCl, 0-5mM $MgCl_2$, and 3mM $ZnCl_2$. Five - ten μl of this solution was deposited on freshly cleaved mica. The samples were allowed to dry for 10-30 minutes, then washed first with water, then 50% ethanol, and finally ethanol. After drying overnight in a vacuum desiccator, imaging was carried out on a Nanoscope III multimode AFM system (Digital Instruments).

Absorbance spectra were performed on an Utrospec 200 UV/Visible spectrophotometer from Pharmacia Biotech using Swift II software.